

Revised 8 February 2024

6 Recording, information transduction, and activation of neurons

6.1 Conceptual fundamentals

6.1.1 Electrical

Electrode measurements are limited by the thermal noise at the electrode surface. This can be expressed by the Johnson noise formula for noise voltage δV , i.e.,

$$\delta V = \sqrt{4k_B T R \Delta\nu} \quad (6.1)$$

where R is the resistance and $\Delta\nu$ is the bandwidth of the amplifier. For a scenario in which the noise is 10-times less than that of the $20\mu V$ intracellular membrane noise and the bandwidth matches that of the rise time of the action potential, requiring $\Delta\nu = 10$ kHz, we find $R \simeq 200$ M Ω . This reflects the reality for intracellular electrodes. A patch electrode can have considerable less resistance, maybe $R \approx 200$ k Ω .

The second issue is the the voltage probe should not draw any current, which is to say that the resistance should be large. This means that the amplifier used with the electrode must have an input resistance large compared to the electrode resistance, on the the range of tens of $G\Omega$ ms; this is reasonable with FET-input amplifiers. In general, the impedance of the probe must be large compared to that of the source - or system under study - to avoid perturbing the source.

6.1.2 Optical

Measurements of light, such as that emitted from a fluorescent source, are limited by the Poisson arrival statistics of photons. Achieving this limits requires that all systematic noise sources, such as an excitation light, are minimized. Shot noise is expressed as a current δI , i.e.,

$$\delta I = \sqrt{2eI\Delta\nu} \quad (6.2)$$

where e is the electronic charge and I is the total current. Typically, the signal one is measuring corresponds of a change in the intensity of light, of a change in I denoted ΔI . Then the signal-to-noise ratio (SNR) is

$$\begin{aligned} SNR &= \frac{\Delta I}{\delta I} \\ &= \frac{\Delta I}{I} \sqrt{\frac{I}{2e\Delta\nu}}. \end{aligned} \quad (6.3)$$

This is an important and telling formula. It states that the SNR varies as the fraction change of the indicator - say a popular calcium indicator like GCaMP - times the square-root of the intensity of the light. We can turn this into numbers of photons, n ,

$$SNR = \frac{\Delta n}{n} \sqrt{n} \quad (6.4)$$

which clearly states that smaller signals require more photons or more measurements to achieve a reliable estimate.

6.1.3 Information and SNR

When does one stop making measurements? We saw (Eq 6.4) that the signal-to-noise increases as we make more and more measurements. So when do we stop? A principled way to think about this is in terms of the transfer of information about the system from a measurement. Here the noise may also include terms from the biological system and various technological sources in addition to fundamentals such as shot noise. Nonetheless, for specific models of the noise, we can calculate the information gained about a system from the measurements. For the case of a measure called mutual information, denoted I_M , and noise assumed to follow Gaussian statistics, which is reasonable for large numbers of measurements, we have a classic result (Box 1) is

$$I_M = \frac{1}{2} \log [1 + (SNR)^2] \quad (6.5)$$

where the square occurs because we need to convert to power, e.g., (voltage)². This states that the mutual information rises linearly when the SNR is small, i.e., $I_M \simeq SNR/2$ (recall $\ln(1+x) \approx x$ for $x \ll 1$), and then rises only slowly for when the SNR becomes large, i.e., $I_M \simeq \log(SNR)$. So, if experimental time is limited and many sites need to be observed, one should only measure until the SNR reaches say 10-ish, then move on!

Box 1. Mutual Information and signal-to-noise

We start with the definition of conditional probability. Let $P(r|s)$ be defined as the probability of a response r given a stimulus s . Then the associated Shannon information, denoted H , or equivalently the entropy of the response, is

$$H(r, s) = - \int dr P(r|s) \log P(r|s) \quad (6.6)$$

The question is if this is larger than a random response. This leads to the definition of the noise entropy, denoted H_{noise} , as an average entropy over all stimuli. Thus

$$\begin{aligned} H_{noise}(r, s) &= \int ds P(s) H(r, s) \\ &= - \int \int ds dr P(s) P(r|s) \log P(r|s) \end{aligned} \quad (6.7)$$

The difference between the entropy of the response, denoted $H_s(r)$ where

$$H(r) = - \int dr P(r) \log P(r) \quad (6.8)$$

and $H_{noise}(r, s)$ is the a measure of what can be gleamed about the stimulus from the response. This is known as the mutual information, denoted I_m , where

$$\begin{aligned} I_M &= H(r) - H_{noise}(r, s) \\ &= - \int dr P(r) \log P(r) + \int \int ds dr P(s)P(r|s) \log P(r|s) \end{aligned} \quad (6.9)$$

To simply this, we know that we can express $P(r)$ and a sum the conditional probability $P(r|s)$ summed over all stimuli, or

$$P(r) = - \int dr P(r|s)P(s) \quad (6.10)$$

Then

$$\begin{aligned} I_M &= - \int \int dr ds P(r|s)P(s) \log P(r) + \int \int ds dr P(s)P(r|s) \log P(r|s) \\ &= \int \int ds dr P(r|s)P(s) \log \frac{P(r|s)}{P(r)} \end{aligned} \quad (6.11)$$

We can go one more step and express this in terms of the joint probability $P(r, s)$, where

$$\begin{aligned} P(r, s) &= P(r|s)P(s) \\ &\text{or} \\ P(r, s) &= P(s|r)P(r). \end{aligned} \quad (6.12)$$

Then

$$I_M = \int \int ds dr P(r, s) \log \frac{P(r, s)}{P(r) P(s)} \quad (6.13)$$

which is zero if the stimulus and the response are uncorrelated, i.e., if $P(r, s) = P(r) P(s)$. Note the alternate expressions (useful below)

$$\begin{aligned} I_M &= \int \int ds dr P(r, s) \log \frac{P(r|s)}{P(r)} \\ &\text{or} \\ I_M &= \int \int ds dr P(r, s) \log \frac{P(s|r)}{P(s)}. \end{aligned} \quad (6.14)$$

Let's calculate the mutual information when the stimulus and response both can be modeled as Gaussian random variables.

- Linear response gives

$$r = Gs + \eta \quad (6.15)$$

where G is the gain of the transduce and η is the additive noise of the transducer, with variance σ^2 . This is the output noise of the system; the noise referred to the input is σ^2/G^2 .

- Let the stimulus s have an average of $\langle s \rangle = 0$ and a variance $\langle s^2 \rangle$. Here $\langle s^2 \rangle$ is the signal, i.e., the mean-square of changes in the input about the mean.

- Let the response r , or output of the transducer, have an average of $\langle r \rangle = 0$ and a variance $\langle r^2 \rangle$. The probability distribution for the response is

$$P(r) = \frac{1}{\sqrt{2\pi \langle r^2 \rangle}} e^{-r^2/2\langle r^2 \rangle} \quad (6.16)$$

Using the notation

$$\langle f(r) \rangle \equiv \int dr P(r) f(r) \quad (6.17)$$

The entropy $H(r)$ of this distribution is

$$\begin{aligned} H(r) &= -\langle \log P(r) \rangle \\ &= -\frac{1}{\ln 2} \left\langle \frac{1}{2} \ln (2\pi \langle r^2 \rangle) + \frac{r^2}{2 \langle r^2 \rangle} \right\rangle \\ &= -\frac{1}{\ln 2} \left[\frac{1}{2} \ln (2\pi \langle r^2 \rangle) + \frac{\langle r^2 \rangle}{2 \langle r^2 \rangle} \right] \\ &= -\frac{1}{2 \ln 2} \left[\ln (2\pi \langle r^2 \rangle) + 1 \right] \end{aligned} \quad (6.18)$$

where we used $\log_2 x = (1/\ln 2) \ln x$.

Lets now consider the conditional probability of the response given the stimulus, i.e.,

$$P(r|s) = \frac{1}{\sqrt{2\pi\sigma^2}} e^{-(r-Gs)^2/2\sigma^2} \quad (6.19)$$

where Gs is the mean response. Using the previous notation

$$\langle f(r) \rangle \equiv \int dr P(r, s) f(r) \quad (6.20)$$

and the alternate form for I_M (Eq 6.15), we have

$$\begin{aligned} I_M &= \left\langle \log \frac{P(r|s)}{P(r)} \right\rangle \\ &= \frac{1}{\ln 2} \left[-\frac{1}{2} \ln (2\pi\sigma^2) + \frac{1}{2} \ln (2\pi \langle r^2 \rangle) - \frac{\langle (r - Gs)^2 \rangle}{2\sigma^2} + \frac{\langle r^2 \rangle}{2 \langle r^2 \rangle} \right] \\ &= -\frac{1}{2 \ln 2} \left(\ln \frac{\langle r^2 \rangle}{\sigma^2} - \frac{\langle \sigma^2 \rangle}{\sigma^2} + \frac{\langle r^2 \rangle}{\langle r^2 \rangle} \right) \\ &= -\frac{1}{2 \ln 2} \ln \frac{G^2 \langle s^2 \rangle + \sigma^2}{\sigma^2} \end{aligned} \quad (6.22)$$

where we used $\langle r^2 \rangle = G^2 \langle s^2 \rangle + \sigma^2$ since $\langle s \eta \rangle = 0$ and $\langle \eta^2 \rangle \equiv \sigma^2$. Then

$$I_M = \frac{1}{2} \log \left(1 + \frac{\langle s^2 \rangle}{\sigma^2/G^2} \right) \quad (6.23)$$

Recall that σ^2/G^2 is the noise power referred the input, so this is in the form of the general relation $I_M = (1/2) \log [1 + (SNR)^2]$, where the signal-to-noise ratio is the quotient of the standard deviation of the signal to the standard deviation of the noise at the input.

6.2 Modern twists on classical techniques

Classical intracellular recording makes use of glass cylindrical electrodes that provide an intracellular connection to a cell. The modern twist is intracellular recording from a cortical or hippocampal neurons in a mouse that is running on a maze (Figure 1). This shows, for example, that neurons can have so much excitatory drive at the center of their receptive field that the cell is essentially shunted (Figure 2); this phenomena would be missed by extracellular electrodes.

Figure 1: Head-mount for jerk-free insertion of an electrode into a pyramidal cell. From Lee, Manns, Sakmann and Brecht, 2006

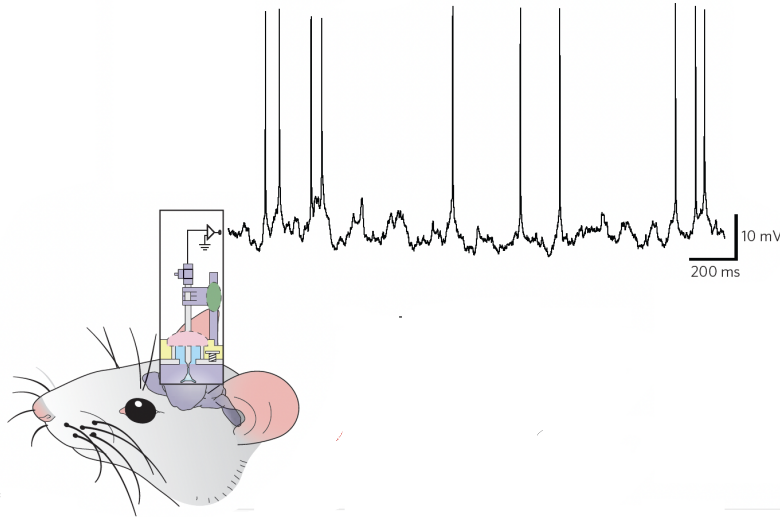
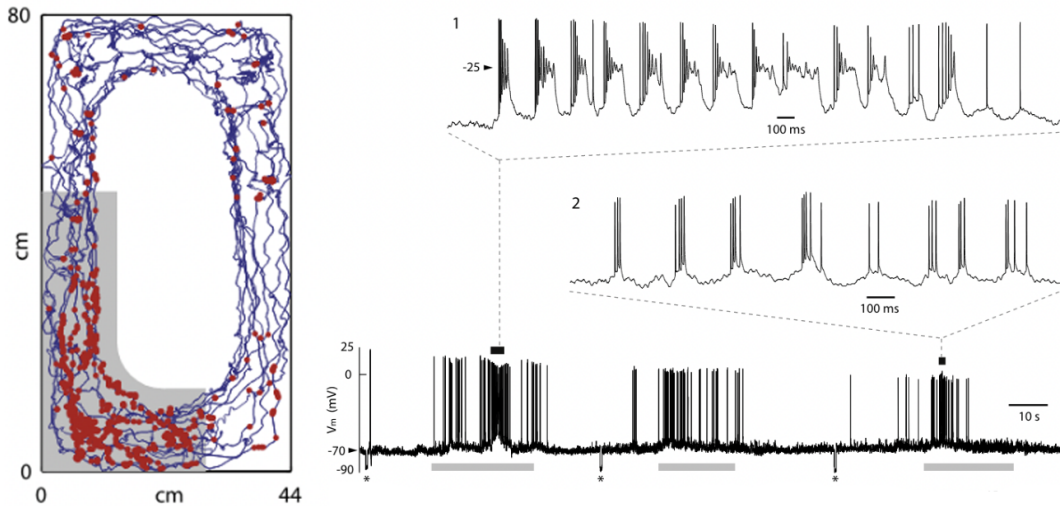


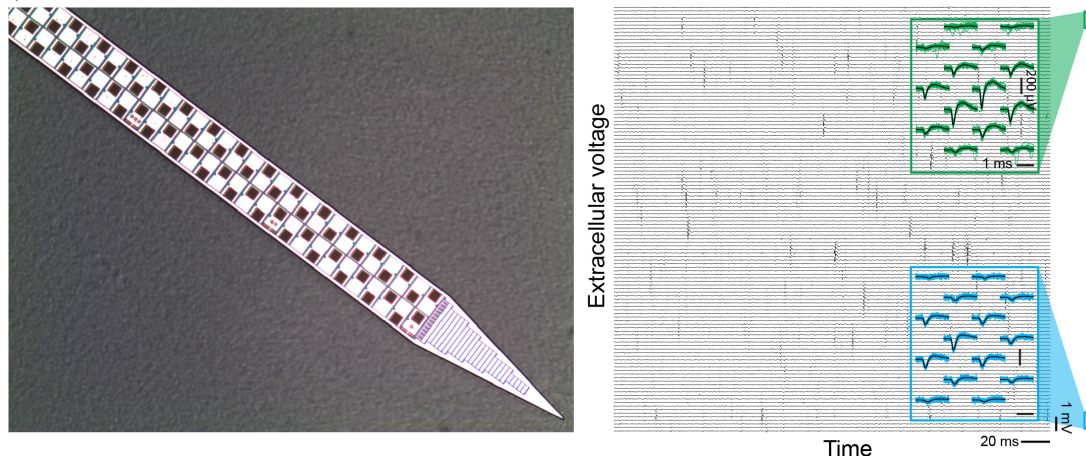
Figure 2: Recording from neurons in CA1 of hippocampus as the mouse passes through its place field; bursts of spikes occurred at regions marked by red dots. From Epsztein, Brecht and Lee, 2011



Classical extracellular recording makes use of metal electrodes that record the flow of

current outside of a cell and provide a means to infer spikes in a neighboring cell. The modern twist is extracellular recording from hundreds of sites at once (Figure 3).

Figure 3: Recording from cortex with Neuropixels. From Jun, Steinmetz, Siegle, Denman, Bauza, Barbarits, Lee, Anastassiou, Andrei, Aydon, Barbic, Blanche, Bonin, Couto, Dutta, Gratiy, Gutnisky, Hausser, Karsh, Ledochowitsch, Lopez, Mitelut, Musa, Okun, Pachitariu, Putzeys, Rich, Rossant, Sun, Svoboda, Carandini, Harris, Koch, O’Keefe and Harris, 2017



6.3 Genetically expressed optical-based indicators of intracellular Ca^{2+} .

In a program started by the late Roger Tsien, these molecules (Figure 6.3) are expressed in vivo in specific cell types and initiate an increase in fluorescence in response to the Ca^{2+} influx that follows an action potential (Figure 5).

Figure 4: The cyclically permutable GFP turned into a detector of intracellular Ca^{2+} . From Chen, Wardill, Sun, Pulver, Renninger, Baohan, Schreiter, Kerr, Orger, Jayaraman, Looger, Svoboda and Kim, 2013.

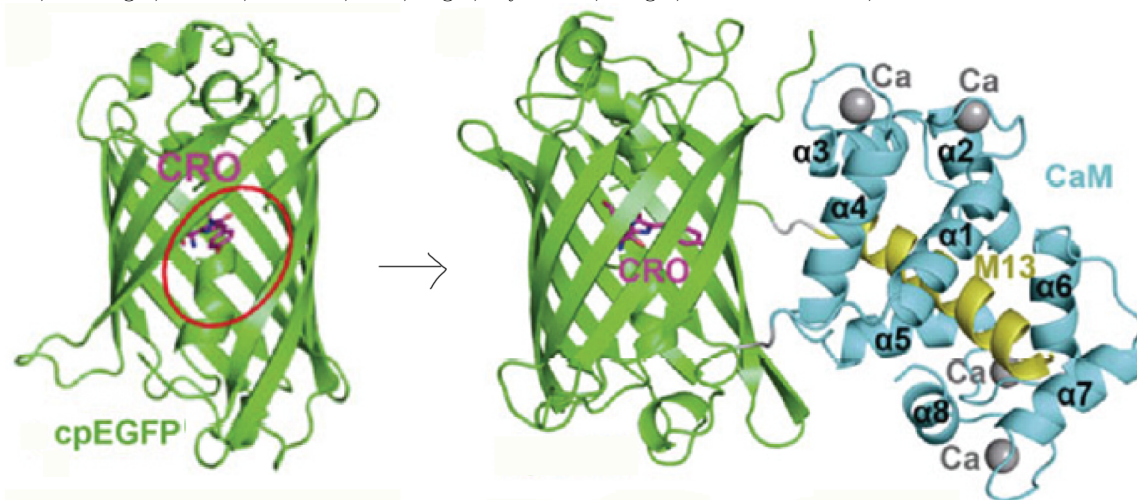
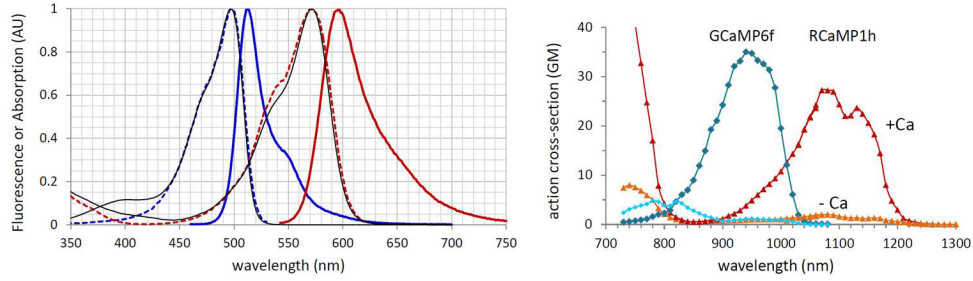


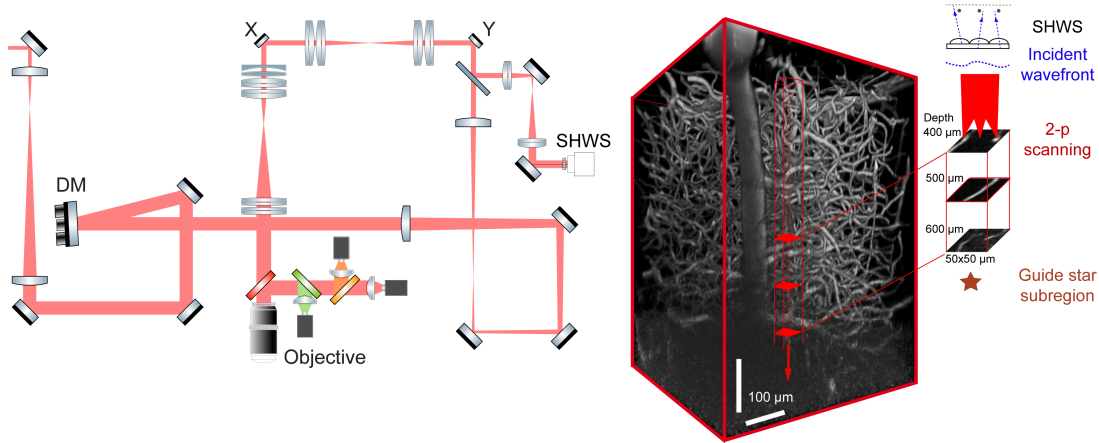
Figure 5: Absorption and fluorescent spectrum.



6.4 In vivo recording of neuronal structure and function with two-photon laser scanning microscopy

Winfried Denk's technique of two-photon laser scanning microscopy, properly pushed to the limit with corrections for the wavefront distortion through tissue (Figure 6), allows changes in intracellular Ca^{2+} to be measured in neuronal soma down to spines in nearly all layers of cortex. Note that the region of observation, the point spread function, is elongated in "z" (Figure 7).

Figure 6: Essential components of a state-of-the-art two photon microscope. From Liu, Li, Marvin and Kleinfeld 2019. Cy5.5-dextran labeled vasculature imaged at $1.25 \mu\text{m}$



6.5 In vivo recording of calcium signaling with two-photon laser scanning microscopy

In vivo Ca^{2+} signals may be recorded after a single spike, and from many sites (Figure 8). Still the interpretation in terms of numbers of spikes is imperfect and thus curation is suggested in quantitative interpretation of signals (Figures 6.5, 10, and 11).

Figure 7: The distortion of cell images by the point spread function is most severe along the optical axis. From Tsai, Mateo, Field, Schaffer, Anderson and Kleinfeld, 2015.

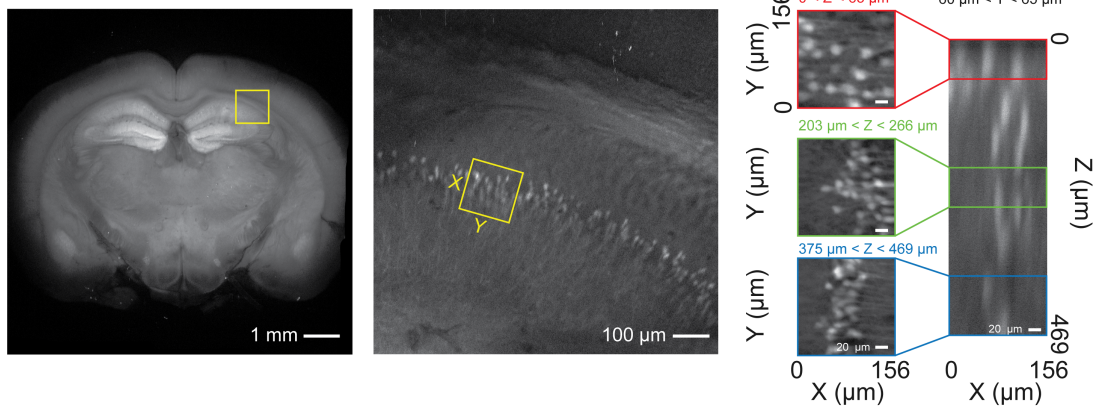


Figure 8: Intracellular responses in superficial V1 of mouse visual cortex using GCaMP6. From Chen, Wardill, Sun, Pulver, Renninger, Baohan, Schreier, Kerr, Orger, Jayaraman, Looger, Svoboda and Kim, 2019.

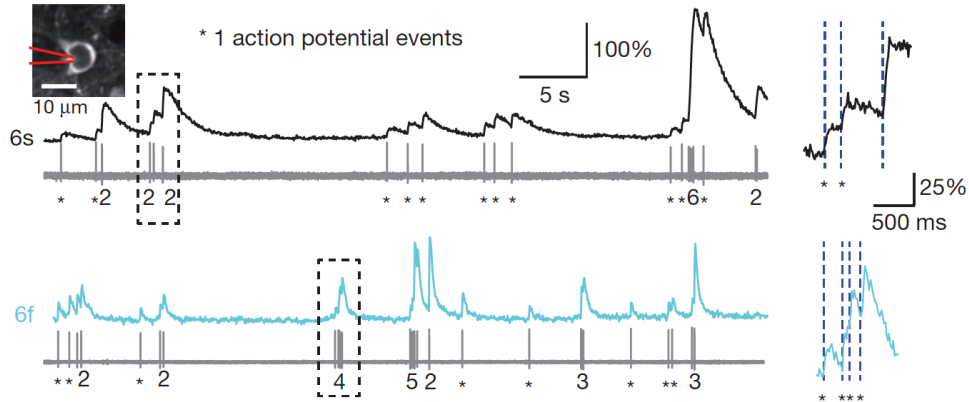


Figure 9: Intracellular responses in hippocampal brain slice with cell culture using Oregon Green BABTA. From Sasaki, Takahashi, Matsuki and Ikegaya, 2008.

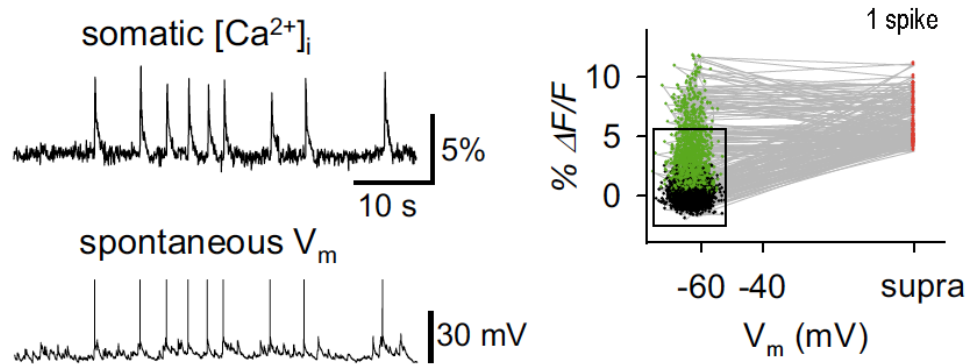


Figure 10: Intracellular Ca^{2+} is an unreliable measure of spike count and may fail to detect single spikes in vivo. From Theis, Berens, Froudarakis, Reimer, Roson, Baden, Euler, Tolias and Bethge 2016.

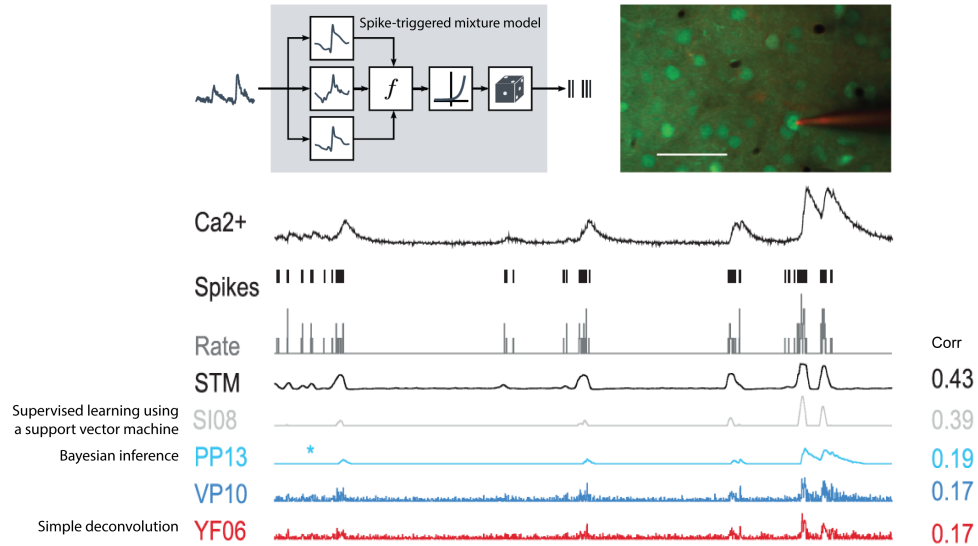
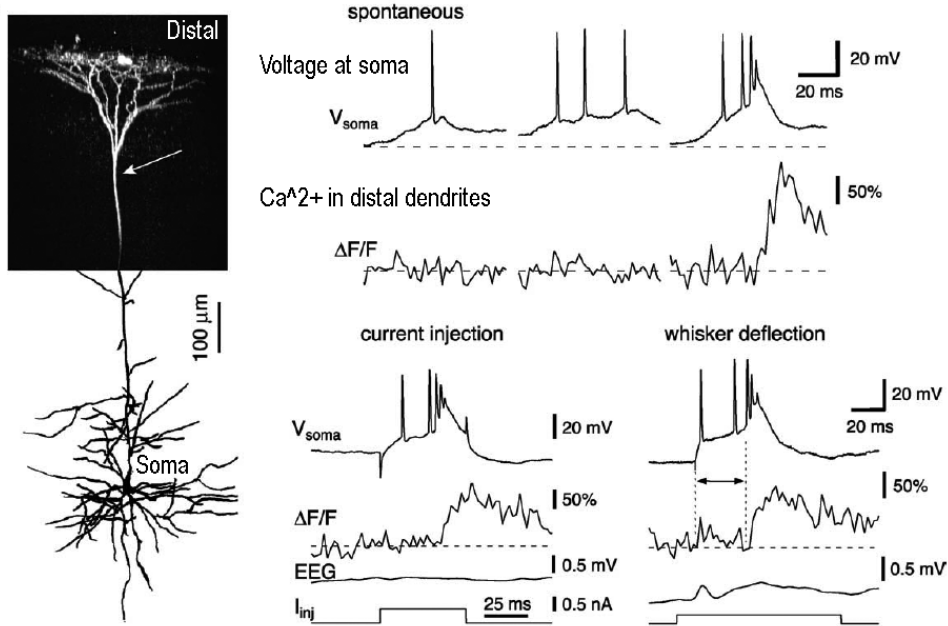


Figure 11: Intracellular Ca^{2+} in distal dendrites of L5b neurons can dissociate from somatic electrical activity. From Helmchen and Waters 2002.



6.6 In vivo recording of activity in the locomoting animal

The use of virtual reality in combination with two-photon microscopy permits behavior and circuit dynamics to be concurrently measured (Figures 12 and 13).

Figure 12: In vivo hippocampus preparation. From Dombeck, Harvey, Tian, Looger and Tank 2010.

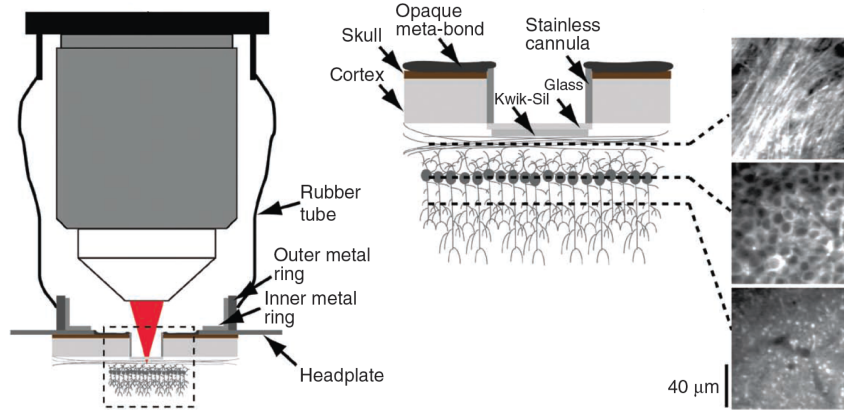
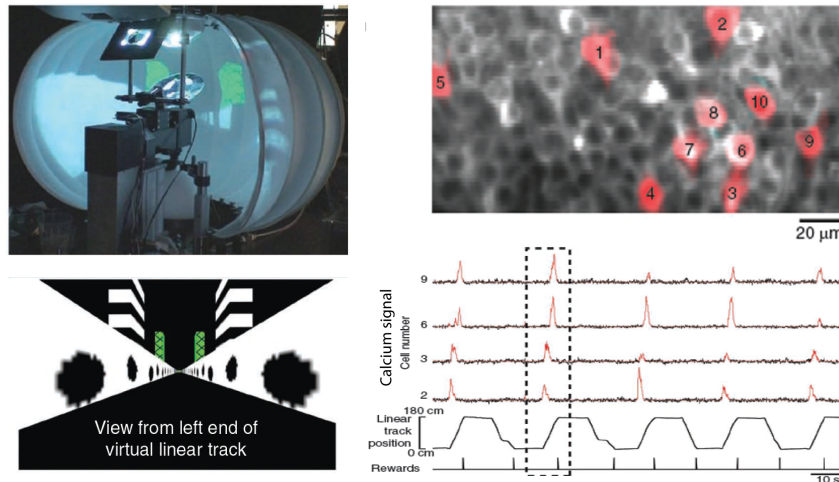


Figure 13: In vivo recording in hippocampus. From Dombeck, Harvey, Tian, Looger and Tank 2010.



6.7 Genetically expressed optical-based drivers of spiking

Optical activation of certain microbial opsin expressed in the membrane of neurons (Figure 14), most famously channelrhodopsin (Figure 15), can be used to photo-excite, or photo-inhibit, neurons.

6.8 All optical schemes for feedback control of spiking

The use of two-photon imaging and concurrent two-photon photoactivation permits behavior and circuit dynamics to be concurrently measured and perturbed solely with light and light-activated molecules (Figures 16, 17, 18, 19, and 20).

Figure 14: Natural transmembrane proteins that use light to pump ion or open ion selective pores.

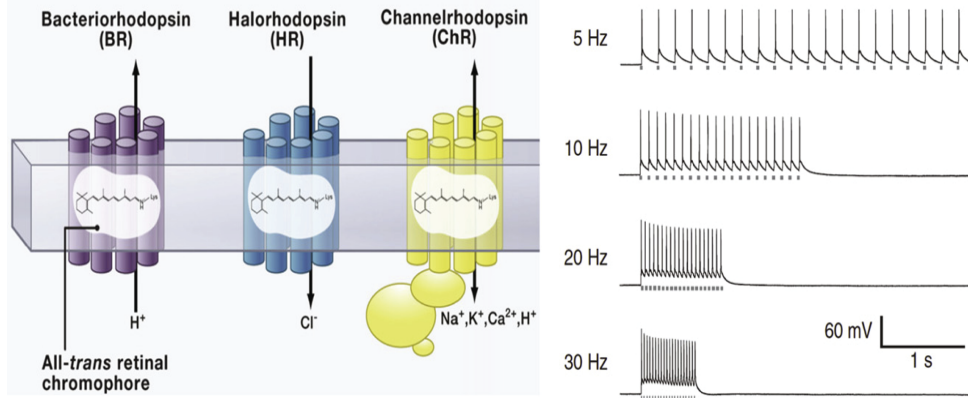


Figure 15: One photon absorption and dynamics of channelrhodopsin. From Klapoetke, Murata, Kim, Pulver, Birdsey-Benson, Cho, Morimoto, Chuong, Carpenter, Tian, Wang, Xie, Yan, Zhang, Chow, Surek, Melkonian, Jayaraman, Constantine-Paton, Wong and Boyden, 2014

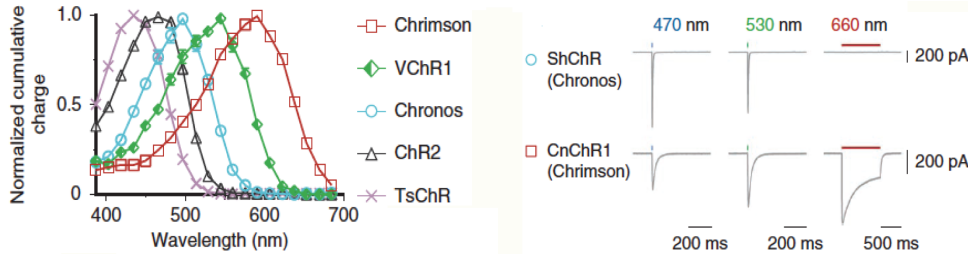


Figure 16: Two-photon action spectra for activating neurons with red-shifted channelrhodopsin C1V1 and action spectrum for recording Ca²⁺ transients with GCaMP3.

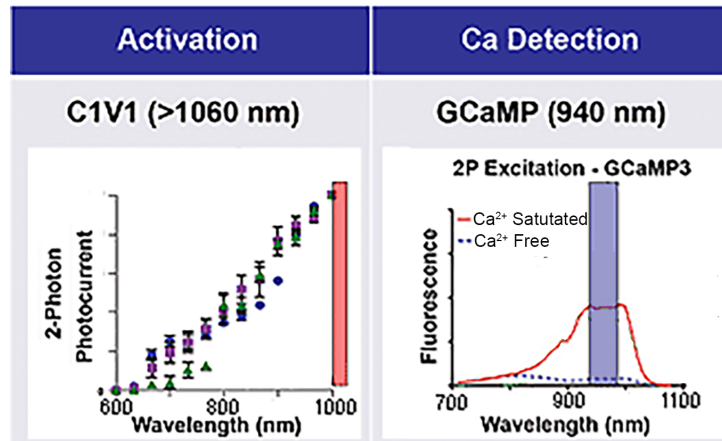


Figure 17: Narrow range of excitation for two-photon activation with red-shifted channelrhodopsin ReaChR. From Chaigneau, onzitti, Gajowa, Soler-Llavina, Tanese, Brureau, Papagiakoumou, Zeng and Emiliani, 2016

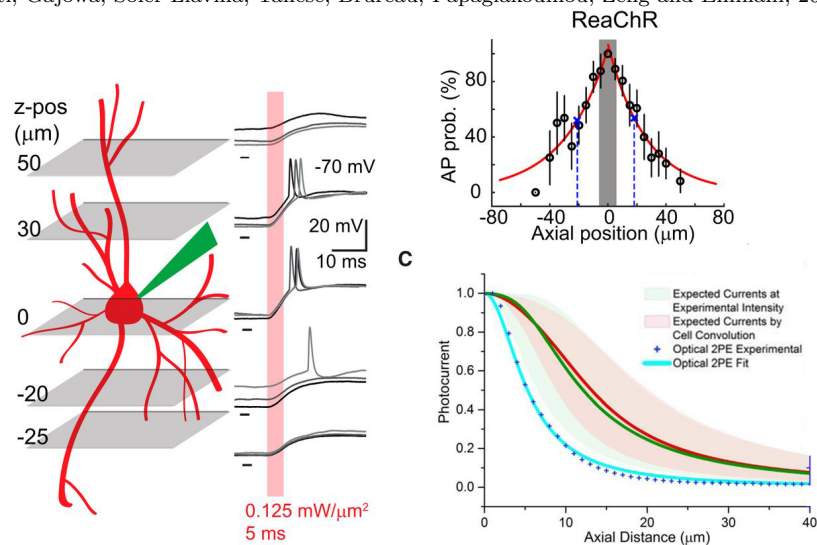


Figure 18: Schematic for feedback induced long-term synaptic potentiation. From Zhang, Russell, Packer, Gauld and Hausser 2018.

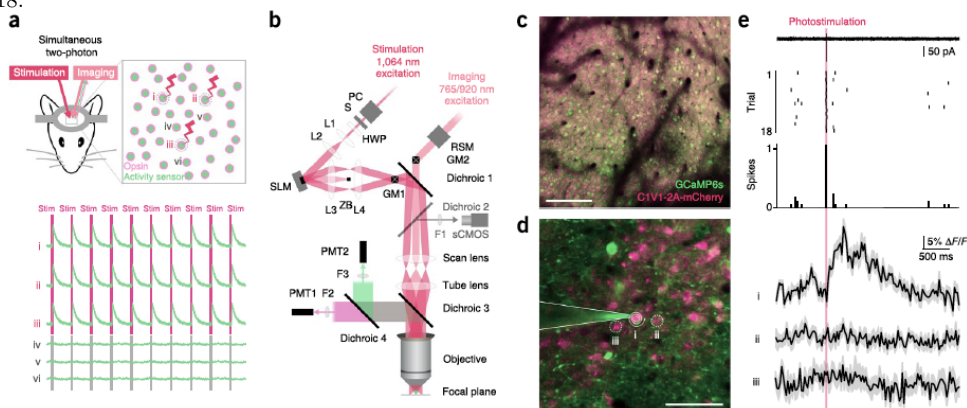


Figure 19: Test of feedback induced long-term synaptic potentiation. From Zhang, Russell, Packer, Gauld and Hausser 2018.

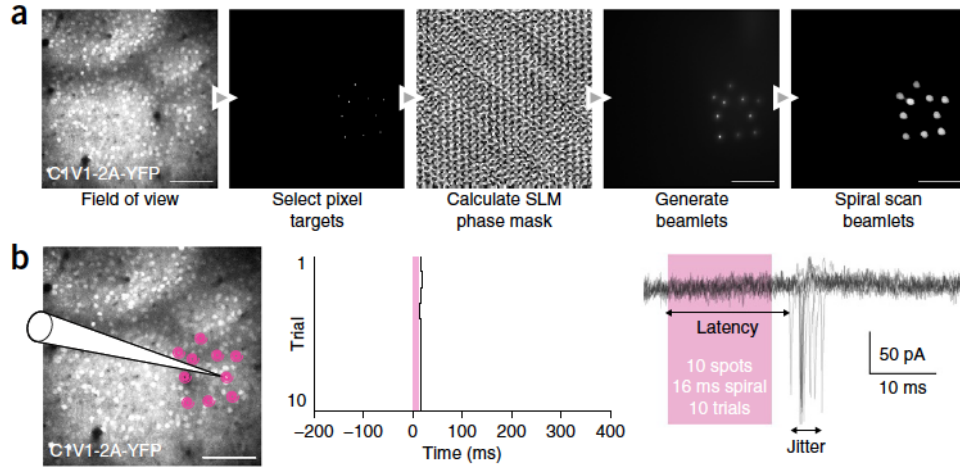


Figure 20: Test of feedback induced long-term synaptic potentiation. From Zhang, Russell, Packer, Gauld and Hausser 2018.

